ARTICLE TYPE

Mechanized Silica Nanoparticles Based on Reversible Bistable [2]Pseudorotaxanes as Supramolecular Nanovalves for Multistage pH-Controlled Release

**MingDong Wang,‡ Tao Chen,‡ ChenDi Ding and JiaJun Fu***

Cucurbit[6]uril-based reversible bistable [2]pseudorotaxanes were designed, synthesized and installed on the surface of mesoporous silica nanoparticles as supramolecular
10 **nanovalves. The assembled mechanized silica nanoparticles realize the multistage pH-controlled release of benzotriazole and the potential for reutilization.**

Mechanized silica nanoparticles (MSNPs), which are composed of mesoporous silica nanoparticles as scaffolds and mechanically
15 interlocked molecules as supramolecular nanovalves, are capable of accommodating and releasing cargo molecules on demand and have received great attention due to their potential applications in the field of stimuli-responsive controlled drug delivery systems and intelligent anticorrosion coatings.[1,2] As the key part of
20 MSNPs, supramolecular nanovalves usually in the form of [2]pseudorotaxanes and bistable [2]rotaxanes undergo the relative mechanical movement between their ring components and threads on the nanoscale, by which MSNPs can encapsulate the cargo molecules within the mesopores under normal conditions
25 and release in response to environmental changes, such as pH, redox potential, light and biomolecules, *etc*.[3-6]

In the past decade, a multitude of supramolecular nanovalves based on [2]pseudorotaxanes have been designed and fabricated. The transition states of nanovalves from "closed" to "open" are
30 mainly caused by the gradually weak supramolecular interactions between the macrocycles and the linear stalks anchored on the surface of mesoporous silica nanoparticles upon external stimuli. However, after accomplishing release missions, the complete structures of MSNPs are broken owing to the dethreading of
35 macrocyclic gatekeepers from the linear stalks.[7] As comparison, making use of bistable [2]rotaxanes as nanovalves not only actualizes multistage controlled release in a way of "release-halt-release", but also achieves another important objective for reloading and reusing of MSNPs by the reciprocating motion of
40 macrocycles on the linear stalks. To our knowledge, the investigations of bistable [2]rotaxanes to realize reversible switching function are still rare. Stoddart and Zink *et al.* attached the bistable [2]rotaxanes covalently to the surface of MCM-41 and finish a cycle for loading and releasing of guest molecules, in
45 which cyclobis(paraquat-*p*-phenylene) (CBPQT[4+]) macrocycles shuttled between the tetrathiafulvalene (TTF) stations and the dioxynaphthalene (DNP) stations under redox control.[8] Lately,

they have designed light-triggered reversible nanovalves based on azobenzene α-cyclodextrin system.[9]
50   Herein, we introduce a novel design for MSNPs based on mesoporous silica nanoparticles equipped with the reversible bistable [2]pseudorotaxanes to control pore access. The molecular structure of the bistable [2]pseudorotaxane, which contains 1,6-hexanediammonium (HDA) and 1,6-bis(pyridinium)hexane (BPH)
55 as two recognition sites, as well as cucurbit[6]uril (CB[6]) as macrocycles are shown in Scheme 1. In this interlocked molecule, CB[6] macrocycles can be switched between two distinct recognition sites according to pH changes. Under neutral or acidic solution, the CB[6] macrocycles choose to stay on the
60 HDA stations rather than the BPH stations, preventing cargo molecules escape. When the pH value turns to alkaline, the ammonium moieties of HDA are deprotonated and the binding affinity between CB[6] macrocycles and HDA stations is weakened, which leads to the migration of CB[6] macrocycles
65 from the HDA recognition stations to the BPH stations far away from the entrance of pores. At this moment, the nanovalves are opened and the cargo molecules are free to diffuse out. If the pH of solution is adjusted from alkaline to weak acidic condition once more, the CB[6] macrocycles originally recognized on the
70 BPH stations will shuttle back to the HDA stations, which facilitates the well-designed MSNPs fulfil the multistage
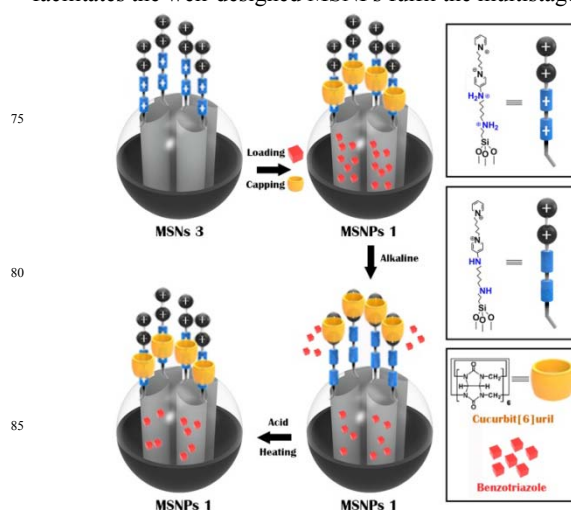
Scheme 1. Schematic representation of operation of the MSNPs **1**.

pH-controlled release and therefore, can be recycled and reused.

MCM-41-type mesoporous silica nanoparticles (MSNs) were synthesized according to the previous literature and used as stating nanocarriers.[10] Transmission electron microscopy, small-angle X-ray powder diffraction, and N_2 adsorption-desorption isotherms characterize that the monodispersed, diameter of about 150 nm nanospheres have a hexagonal channels with a 2.65 nm average pore diameter and a surface area of 1118 m^2 g^{-1} (Fig. S2, ESI†). The assembly process of MSNP **1** is depicted in Fig. S1 (ESI†). The as-prepared MSNs were firstly functionalized with (3-aminopropyl) trimethoxysilane to obtain MSNs **1**, which were then treated with 1,6-dibromohexane to give MSNs **2**. After that, the MSNs **2** were reacted with compound **1** (detailed synthesis process were seen in ESI†) to yield MSNs **3**. To obtain MSNPs **1**, the MSNs **3** were loaded with 1*H*-benzotriazole (BTA), which is chosen as probe molecule and capped with CB[6] macrocycles.

Three-step functionalization processes are confirmed through Fourier Transformed Infrared (FTIR) spectroscopy. As shown in Fig. 1, MSNs only show the various Si-OH and Si-O-Si vibrations, while MSNs **1** exhibit an absorption band at 2930 cm^{-1}, which corresponds to the C-H stretching vibration. Compared with MSNs **1,** a new absorption band at 580 cm^{-1}, a characteristic stretching band of the C-Br bond is shown in the FTIR spectrum of MSNs **2**. After coupled with Compound **1**, the intensity band of C-Br bond is considerably reduced, and the absorption peaks at 1500-1400 cm^{-1} are appeared due to the pyridine skeleton vibration, indicating the successful attachment of organic stalks on the exterior surfaces of MSNs. The ^{13}C CP-MAS solid-state NMR spectrum of MSNs **1**, MSNs **2** and MSNs **3** are illustrated in Fig. 2 and provide further evidence of functionalization. The NMR spectrum of MSNs **1** shows three resonance signals at 10, 26 and 43 ppm that can be attributed to the peaks of carbon *a*, *b*, and *c* of 3-aminopropyl group. In the NMR spectrum of MSNs **2**, apart from the peaks for carbons *a*, *b* and *c*, some new intense signals were observed at 22, 51, 55, 60 ppm, corresponding to the carbons *f-g*, *e-h*, *i* and *d* on hexyl chain. As for MSNs **3**, the additional three resonance signals appearing around 128, 146 and 160 ppm can be assigned to the characteristic aromatic carbon (*k-t*, *l-s-u* and *j*) of the pyridine groups, indicating the formation of the second recognition sites, BPH stations, which is also proved by the ^{29}Si CP-MAS solid-state NMR spectra (Fig. S3, ESI†).
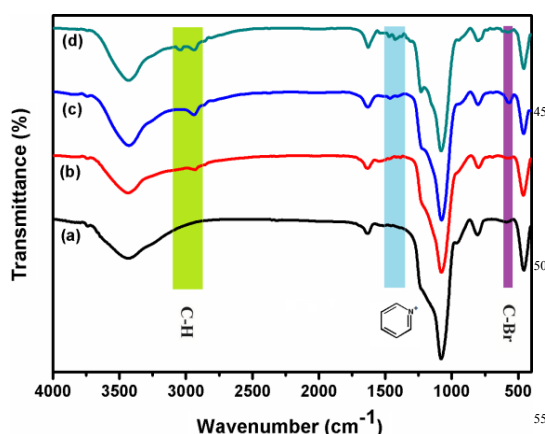

Fig. 1 FTIR spectra of pure MSNs (a), MSNs **1** (b), MSNs **2** (c), and MSNs **3** (d).

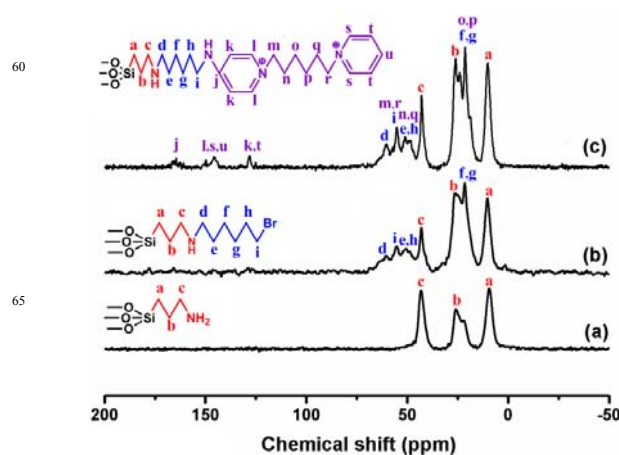**Fig. 2** ^{13}C CP-MAS solid-state NMR spectra of MSNs **1** (a), MSNs **2** (b), and MSNs **3** (c).

The X-ray photoelectron spectroscopy (XPS) is also used to verify the introduction of the intact stalks inside the framework of MSNs. The apparent differences between MSNs **3** and MSNs (Fig. S4, ESI†) are the presence of N 1s and C 1s signals in the XPS spectrum of MSNs **3**, but not detected in the MSNs. From thermogravimetric analysis data as shown in Fig. S5 (ESI†), when MSNs are successively functionalized with (3-aminopropyl) trimethoxysilane, 1,6-dibromohexane and Compound **1**, the approximate total weight loss is 11.5 wt% (about 0.86 mmol g^{-1} MSNs), 8.5 wt% (about 0.5 mmol g^{-1} MSNs), and 7.4 wt% (about 0.42 mmol g^{-1} MSNs), respectively. Although the intensity of diffraction peak, the specific surface area and the pore volume are inevitably decreased after each step of functionalization, this does not greatly influence the adsorption capacity of mesoporous materials (Fig. S6 and Fig. S7, ESI†).

After installation the planned stalks, the MSNPs **1** were assembled. The three different measurement methods were adopted to investigate the operation modes of MSNP **1** in detail. First of all, Fig. 3 shows release profiles by plotting the absorbance intensity of BTA at 265 nm from the MSNPs **1** in response to different pH as a function of time. The leakage of BTA at pH 7.0 was negligible (less than 1.2% total amount of the adsorbed BTA), revealing that the entrance of pores were blocked by CB[6] macrocycles. But in the alkaline solution, the UV/Vis absorbance of BTA increased immediately, manifesting the rapid escape of BTA from MSNPs **1**. Furthermore, the release rate is obviously dependent on the alkalinity of solution. The stronger the alkalinity is, the higher deprotonation degree of HDA units is, the more numbers of CB[6] macrocycles detached from the HDA stations there are, and the more rapid release rate we observe.

In the condition of near neutral or acidic solution, CB[6] macrocycles are threaded onto the HDA stations due to that the stability constant for the host-guest complex between CB[6] and HDA units is more than that between CB[6] and BPH units.[11] As solution alkalinity is increased, 1,6-hexanediammonium are gradually in the deprotonated form.[12] The high binding affinity of complex HDA ⊂ CB[6] dramatically declines, the CB[6] macrocycles cannot reside on the HDA stations and transfer to the BPH stations where the complex formation of BPH⊂CB[6] is little affected by pH values. In order to validate the reversibility of the moving process of CB[6] macrocycles, the second step,
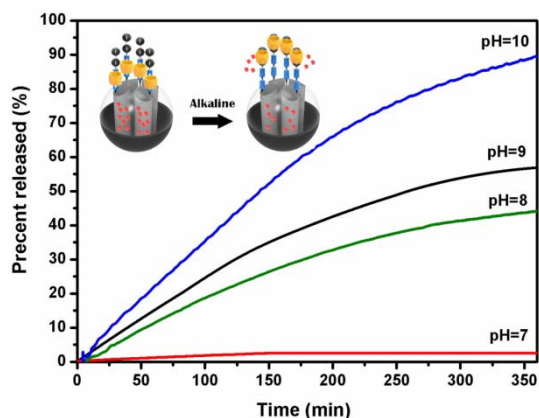
Fig. 3 Release profiles of BTA from MSNPs **1** at different pH values.

the multistage pH-controlled release experiment was conducted. As depicted in Fig. 4a, there was almost no leakage of BTA under
[5] pH 4.5. When the releasing process lasted for 60 min under pH 9.5, the pH of solution was readjusted to 4.5, simultaneously supplemented by heating solution to 45 ℃ for 2 h. After that, the release process was found to be shut off and the concentration of benzotriazole in solution was very stable through continuous
[10] monitoring, demonstrating that CB[6] macrocycles shuttled back to the HDA stations and restarted to regulate the guest molecules diffusing in or out of the MSNPs **1**.

Based on the anticipative results of the multistage pH-controlled experiment, the reloading ability of MSNPs **1** was
[15] finally investigated. The approximately complete release of BTA was performed at pH 10.5 for 12 h. The reloading procedure is similar to the initial adsorption experiment. The re-collected MSNPs **1** were suspended in 15 mg mL^{-1} aqueous BTA solution at pH 10.5 for 12 h, which ensures the encirclement of CB[6]
[20] macrocycles on the BPH stations during the reloading process, and then closed the nanovalves, washed for the second release measurement. As shown in Fig. 4b, the pH-controlled release profile for the second cycle exhibits the similar features as that from the first cycle. However, the reloading capacity is less than
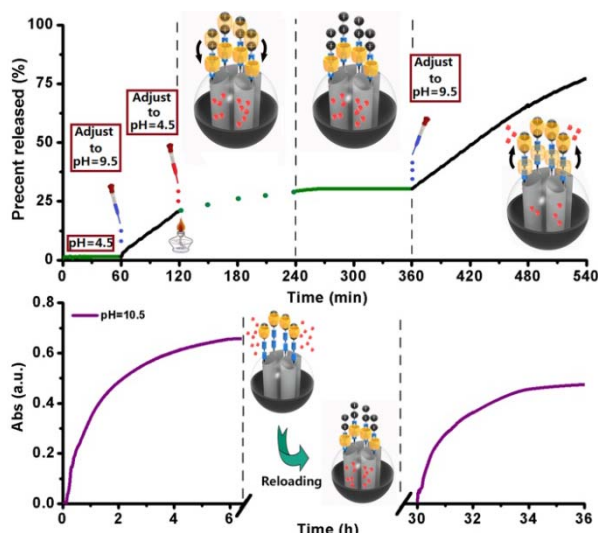[25] 20% for the first cycle, which maybe attributed to the space steric

Fig. 4 Multistage pH-controlled release of BTA from MSNPs **1** (a) and reloading experiment of MSNPs **1** (b).

effect of CB[6] macrocycles.

In summary, a new type of MSNPs with the reversible bistable
[30] [2]pseudorotaxanes as supramolecular nanovalves has been developed. The one-dimensional piston movement of CB[6] macrocycles between the HDA and the BPH stations guarantee the reversible switching activity of nanovalves. The operational mechanisms make MSNPs **1** open or close repeatedly at the
[35] molecular lever in response to pH stimulus, which will expand their application areas.

Notes and references

School of Chemical Engineering, Nanjing University of Science and Technology, Nanjing, China. Fax:+86 025 84315609; Tel: +86 025
[45] *84315609; E-mail: fujiajun668@gmail.com*
† Electronic Supplementary Information (ESI) available: [Experimetal details and analytical data]. See DOI: 10.1039/b000000x/
‡ These authors contributed equally to this article.

1   (a) K. K. Coti, M. E. Belowich, M. Liong, M. W. Ambrogio, Y.A.
[50]   Lau, H. A. Khatib, J. I. Zink, N. M. Khashab and J. F. Stoddart, *Nanoscale*, 2009, **1**, 16; (b) M. W. Ambrogio, C. R. Thomas, Y. L. Zhao, J. I. Zink and J. F. Stoddart, *Acc. Chem. Res.*, 2011, **44**, 903; (c) P. P. Yang, S. L. Gai and J. Lin, *Chem. Soc. Rev.*, 2012, **41**, 3679.
2   (a) T. Chen and J. J. Fu, *Nanotechnology*, 2012, **23**, 235605; (b) T.
[55]   Chen and J. J. Fu, *Nanotechnology*, 2012, **23**, 505705; (c) J. J. Fu, T. Chen, M. D. Wang, N. W. Yang, S. N. Li, Y. Wang and X. D. Liu, *ACS Nano*, 2013, **7**, 11397.
3   (a) M. Xue, X. Zhong, Z. Shaposhnik, Y. Q. Qu, F. Tamanoi, X. F. Duan and J. I. Zink, *J. Am. Chem. Soc.*, 2011, **133**, 8798; (b) Y. L.
[60]   Zhao, Z. X. Li, S. Kabehie, Y. Y. Botros, J. F. Stoddart and J. I. Zink, *J.Am. Chem. Soc.*, 2010, **132**, 13016; (c) S. Angelos, N. M. Khashab, Y. W. Yang, A. Trabolsi, H. A. Khatib, J. F. Stoddart and J. I. Zink, *J. Am.Chem. Soc.*, 2009, **131**, 12912; (d) T. Chen, N. W. Yang, J. J. Fu, *Chem. Commun.*, 2013, **49**, 6555.
[65] 4   (a) R. Liu, X. Zhao, T. Wu and P. Y. Feng, *J. Am. Chem. Soc.*, 2008, **130**, 14418; (b) G. Q. Silveira, M. D. Vargas and C. M. Ronconi, *J. Mater. Chem.*, 2011, **11**, 6034.
5   (a) Y. L. Sun, B. J. Yang, S. X. A. Zhang, Y. W. Yang, *Chem.-Eur. J.*, 2012, **18**, 9212; (b) H. Yan, C. Teh, S. Sreejith, L. L. Zhu, A. Kwok,
[70]   W. Q. Fang, X. Ma, K. T. Nguyen, V. Korzh, Y. L. Zhao, *Angew. Chem.-Int. Edit.*, 2012, **51**, 8373; (c) S. Angelos, Y. W. Yang, N. M. Khashab, J. F. Stoddart and J. I. Zink, *J.Am. Chem. Soc.*, 2009, **131**, 11344.
6   (a) Y. L. Sun, Y. Zhou, Q. L. Li and Y. W. Yang, *Chem. Commun.*,
[75]   2013, **49**, 9033; (b) S. S. Wu, X. Huang and X. Z. Du, *Angew. Chem.-Int. Edit.*, 2013, **52**, 5580.
7   (a)D. P. Ferris, Y. L. Zhao, N. M. Khashab, H. A. Khatib, J. F. Stoddart and J. I. Zink, *J.Am. Chem. Soc.*, 2009, **131**, 1686; (b) C. Wang, Z. X. Li, D. Cao, Y. L. Zhao, J. W. Gaines, O. A. Bozdemir,
[80]   M. W. Ambrogio, M. Frasconi, Y. Y. Botros and J. I. Zink, *Angew. Chem.-Int. Edit.*, 2012, **51**, 5460.
8   (a) T. D. Nguyen, H. R. Tseng, P. C. Celestre, A. H. Flood, Y. Liu, J. F. Stoddart and J. I. Zink, *Proc. Natl. Acad. Sci. U.S.A.*, 2005, **19**, 10029; (b) S. Saha, K. C. F. Leung, T. D. Nguyen, J. F. Stoddart and
[85]   J. I. Zink, *Adv. Funct. Mater.*, 2007, **17**, 685.
9   D. Tarn, D. P. Ferris, J. C. Barnes, M. W. Ambroqio, J. F. Stoddart and J. I. Zink, *Nanoscale*, 2014, **6**, 3335.
10 C. Y. Hong, X. Li and C. Y. Pan, *J. Mater. Chem.*, 2009, **19**, 5155.
11 (a) J. W. Lee, K. P. Kim and K. Kim, *Chem. Commun.*, 2001, **11**,
[90]   1042; (b) L. Yuan, R. B. Wang and D. H. Macartney, *J. Org. Chem.*, 2007, **72**, 4539.
12 (a) J. S. Liu and X. Z. Du, *J. Mater. Chem.*, 2010, **20**, 3642; (b) S. Angelos, Y. W. Yang, K. Patel, J. F. Stoddart and J. I. Zink, *Angew. Chem.-Int. Edit.*, 2008, **47**, 2222.

ChemComm Accepted Manuscript